JOC Article

Mechanism of the Base-Assisted Displacement of Chloride by Alcohol in Sulfinyl Derivatives

David Balcells,[†,‡] Gregori Ujaque,[‡] Inmaculada Fernandez,[§] Noureddine Khiar,[||] and Feliu Maseras*[,†,‡]

Institute of Chemical Research of Catalonia (ICIQ), Avinguda Països Catalans 16, 43007 Tarragona, Catalonia, Spain, Unitat de Química Física, Edifici Cn, Universitat Autònoma de Barcelona, 08193 Bellaterra, Catalonia, Spain, Instituto de Investigaciones Químicas, C.S.I.C−Universidad de Sevilla, c/ Américo Vespucio, s/n., Isla de la Cartuja, 41092 Sevilla, Spain, and Departamento de Química Orgánica y Farmacéutica, Facultad de Farmacia, Universidad de Sevilla, c/ Profesor García González, 2, 41012 Sevilla, Spain

fmaseras@iciq.es

Received March 13, 2006

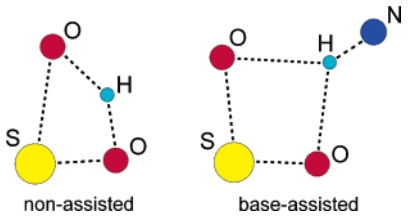

A computational study with density functional theory (DFT) is carried out on the reaction between methyl sulfinyl chloride (MSC) and methanol in the presence of trimethylamine, a process which is a general model for two different methods used in practice for the obtention of chiral sulfoxides through dynamic kinetic resolution. Two mechanistic options are considered: in one of them, chloride is initially displaced by the base (ion pair mechanism), whereas in the other, chloride stays bound to sulfur until its final displacement by methoxy (neutral mechanism). In both cases, the approach of the alcohol to sulfur is coupled with a hydrogen transfer from methanol to the oxo group of MSC in a single concerted transition state. The presence of a trimethylamine molecule facilitates substantially the reaction by reducing the nucleophilic substitution barrier by more than 10 kcal/mol through the formation of a N−H bond with the hydrogen atom being transferred. The neutral mechanism presents a free energy barrier lower than the ion pair alternative and is thus preferred.

Introduction

The synthesis of optically active sulfoxides is a relevant chemical process due to the applications of such compounds in the asymmetric synthesis of biologically active compounds[1] and in metal-assisted asymmetric synthesis.[2] Several synthetic methods have been developed to obtain optically pure sulfoxides.[2,3] Among the most efficient and convenient methods, we find the asymmetric oxidation of prochiral sulfides initially proposed by Bolm,[4] which can be assisted by either vanadium[5−13] or iron,[14,15] and the dynamic kinetic resolution (referred to as

[†] Institute of Chemical Research of Catalonia (ICIQ).
[‡] Universitat Autònoma de Barcelona.
[§] Universidad de Sevilla.
[||] Instituto de Investigaciones Químicas.

(1) Carreño, M. C. *Chem. Rev.* **1995**, *95*, 1717.
(2) Fernández, I.; Khiar, N. *Chem. Rev.* **2003**, *103*, 3651.
(3) Bolm, C.; Muñiz, K.; Hildebrand, J. P. *Comprehensive Asymmetric Catalysis*; Jacobsen, E. N., Pfaltz, A., Yamamoto, H., Eds.; Springer-Verlag: Berlin, 1999; p 697.
(4) Bolm, C.; Bienewald, F. *Angew. Chem., Int. Ed. Engl.* **1995**, *34*, 2640.
(5) Bolm, C.; Schlingloff, G.; Bienewald, F. *J. Mol. Catal. A: Chem.* **1997**, *117*, 347.
(6) Cogan, A. D.; Liu, G.; Kim, K.; Backes, B. J.; Ellman, J. A. *J. Am. Chem. Soc.* **1998**, *120*, 8011.
(7) Plitt, P.; Pritzkow, H.; Krämer, R. *Dalton Trans.* **2004**, 2314.
(8) Skarzewski, J.; Ostrycharz, E.; Siedlecka, R. *Tetrahedron: Asymmetry* **1999**, *10*, 3457.
(9) Bryliakov, K. P.; Karpyshev, S. A.; Fominsky, A. G.; Tolstikov, A. G.; Talsi, E. P.; *J. Mol. Catal. A: Chem.* **2001**, *171*, 73.
(10) Cucciolito, M. E.; Del Litto, R.; Roviello, G.; Ruffo, F. *J. Mol. Catal. A: Chem.* **2005**, *236*, 176.
(11) Zampella, G.; Fantucci, P.; Pecoraro, V. L.; De Gioia, L. *J. Am. Chem. Soc.* **2005**, *127*, 953.
(12) Balcells, D.; Maseras, F.; Lledós, A. *J. Org. Chem.* **2003**, *68*, 4265.
(13) Balcells, D.; Maseras, F.; Ujaque, G. *J. Am. Chem. Soc.* **2005**, *127*, 3624.

10.1021/jo060546p CCC: $33.50
Published on Web 07/27/2006

SCHEME 1. DAG Synthetic Method

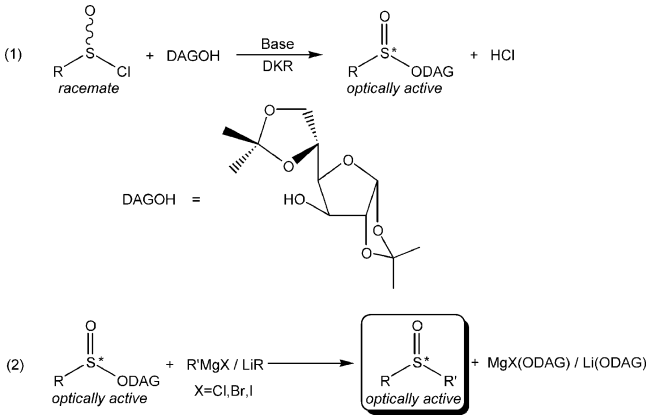

DKR throughout this article) of sulfinyl chlorides,[16−19] initially proposed by Khiar.[20−22] In a recent work, vanadium-assisted oxidation and kinetic resolution have been efficiently combined.[23]

Chiral sulfinate esters are versatile, sulfinylating transfer reagents used to synthesize chiral sulfoxides and sulfinamides.[2] These chiral precursors are obtained by either kinetic or dynamic resolution of sulfinyl chloride racemates. A relevant example of this synthetic methodology is the DAG method developed by some of us[20−22] (see Scheme 1). This method consists of the DKR of a sulfinyl chloride racemate in the presence of stoichiometric amounts of the DAGOH (diacetone-D-glucose) chiral alcohol and an organic nitrogenated base. The reaction implies Cl substitution by DAGO, giving rise to a new S−ODAG bond (step 1 in Scheme 1). The chiral sulfinate ester product reacts with a Grignard reagent in a subsequent step, yielding optically active sulfoxides (step 2 in Scheme 1). This method has been used in the synthesis of structurally diverse sulfoxides with synthetic[24] and pharmacological interest,[25,26] including C_2-symmetric bis-sulfoxides[21,22] that have been used in metal-catalyzed asymmetric synthesis.[27−29] An interesting

SCHEME 2. Cinchona-Assisted DKR of Sulfinyl Chlorides

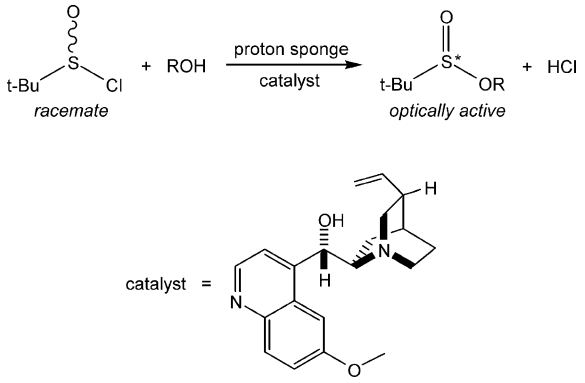

related reaction has been recently reported by Ellman in which nonchiral alcohols are used in combination with optically active bases,[16] usually of the cinchona type,[17] that act as catalysts (an example is given in Scheme 2). The relevant novel contribution of this method is that the only chiral compound needed (the base) is used in small catalytic amounts. As in the DAG method, the final sulfinate ester product can be easily transformed into asymmetric sulfoxides by reaction with Grignard reagents. Both synthetic methods require the presence of some substance able to neutralize the HCl byproduct like an organic base (DAG method) or a proton sponge (cinchona-assisted DKR).

Resolution of racemates is still the most important asymmetric synthesis method in industry.[30−33] In the kinetic resolution, one enantiomer is transformed into the desired reaction product faster than the other.[34,35] However, this method has the important limitation of having a maximum yield of 50%. In contrast with this, both enantiomers of the reactant racemate are somehow interconnected in the DKR methodology,[36−40] and maximum yields of 100% are then possible. In a recent study, we showed that nitrogenated organic bases are able to catalyze the pyramidal inversion of sulfinyl chlorides.[41] The energy barrier for the inversion of SO(Cl)(Me) was found to be reduced from 63.4 kcal/mol (base-free reaction) to 22.9 kcal/mol by NMe_3. The base-assisted inversion of the sulfinyl chloride was thus proposed as a feasible origin of the DKR in the DAG and cinchona-assisted methods. This explains how the two enantiomers of the reactant can interconvert, but the detailed path connecting reactants to products remains unknown. In particular, the role of the base is not fully understood, and its effect on the enantioselectivity of the reaction is critical.

(14) Legros, J.; Bolm, C. *Angew. Chem., Int. Ed.* **2004**, *43*, 4225.
(15) Legros, J.; Bolm, C. *Chem.−Eur. J.* **2005**, *11*, 1086.
(16) Evans, J. W.; Fierman, M. B.; Miller, S. J.; Ellman, J. A. *J. Am. Chem. Soc.* **2004**, *126*, 8134.
(17) (a) Peltier, H. M.; Evans, J. W.; Ellman, J. A. *Org. Lett.* **2005**, *7*, 1733. See also (b) Shibata, N.; Matsunaga, M.; Fukuzumi, T.; Nakamura, S.; Toru, T. *Synlett* **2005**, 1699.
(18) Shibata, N.; Matsunaga, M.; Nakagawa, M.; Fukuzumi, T.; Nakamura, S.; Toru, T. *J. Am. Chem. Soc.* **2005**, *127*, 1374.
(19) Lu, B. Z.; Jin, F.; Zhang, Y.; Wu, X.; Wald, S. A.; Senanayake, C. H. *Org. Lett.* **2005**, *7*, 1465.
(20) Fernández, I.; Khiar, N.; Llera, J. M.; Alcudia, F. *J. Org. Chem.* **1992**, *57*, 6789.
(21) Khiar, N.; Alcudia, F.; Espartero, J.; Rodríguez, L.; Fernández, I. *J. Am. Chem. Soc.* **2000**, *122*, 7598.
(22) Khiar, N.; Araújo, C. S.; Alcudia, F.; Fernández, I. *J. Org. Chem.* **2002**, *67*, 345.
(23) Drago, C.; Caggiano, L.; Jackson, R. F. W. *Angew. Chem., Int. Ed.* **2005**, *44*, 7221.
(24) Carreño, M. C.; García-Ruano, J. L.; Maestro, M. C.; Martín Cabrejas, L. M. *Tetrahedron: Asymmetry* **1993**, *4*, 727.
(25) Zhang, Y.; Talay, P.; Cho, C.-G.; Posner, G. H. *Proc. Natl. Acad. Sci. U.S.A.* **1992**, *89*, 2399.
(26) Parry, R. J.; Li, Y.; Gomez, E. E. *J. Am. Chem. Soc.* **1992**, *114*, 5946.
(27) Khiar, N.; Fernández, I.; Alcudia, F. *Tetrahedron Lett.* **1993**, *34*, 123.
(28) Tokunoh, R.; Sodekoa, M.; Ace, K.; Shibasaki, M. *Tetrahedron Lett.* **1995**, *44*, 8035.
(29) Owens, T. D.; Hollander, F. J.; Oliver, A. G.; Ellman, J. A. *J. Am. Chem. Soc.* **2001**, *123*, 1539.
(30) *Chirality in Industry: The Commercial Manufacture and Applications of Optically Pure Compounds*; Collins, A. N., Sheldrake, G. N., Crosby, J., Eds.; Wiley & Sons: Chichester, 1992.
(31) *Chirality in Industry II: Developments in the Commercial Manufacture and Appliations of Optically Pure Compounds*; Collins, A. N., Sheldrake, G. N., Crosby, J., Eds.; Wiley & Sons: Chichester, 1997.
(32) Sheldon, R. A. *Chirotechnology: Industrial Synthesis of Optically Active Compounds*; Dekker: New York, 1993.
(33) Hawkins, J. M.; Watson, T. J. N. *Angew. Chem., Int. Ed.* **2004**, *43*, 3224.
(34) Chen, C.-S.; Fujimoto, Y.; Girdaukas, G.; Sih, C. J. *J. Am. Chem. Soc.* **1982**, *104*, 7294.
(35) Chen, C.-S.; Fujimoto, Y.; Girdaukas, G.; Sih, C. J. *J. Am. Chem. Soc.* **1987**, *109*, 2812.
(36) Huerta, F. F.; Minidis, A. B. E.; Bäckvall, J. *Chem. Soc. Rev.* **2001**, *30*, 321.
(37) Pellissier, H. *Tetrahedron* **2003**, *59*, 8291.
(38) Caddick, S.; Jenkins, K. *Chem. Soc. Rev.* **1996**, 447.
(39) Sturmer, R. *Angew. Chem., Int. Ed. Engl.* **1997**, *36*, 1173.
(40) Trost, B.; Bunt, R. C.; Lemoine, R. C.; Calkins, T. L. *J. Am. Chem. Soc.* **2000**, *122*, 5968.
(41) Balcells, D.; Maseras, F.; Khiar, N. *Org. Lett.* **2004**, *6*, 2197.

SCHEME 3. Addition/Elimination Mechanisms

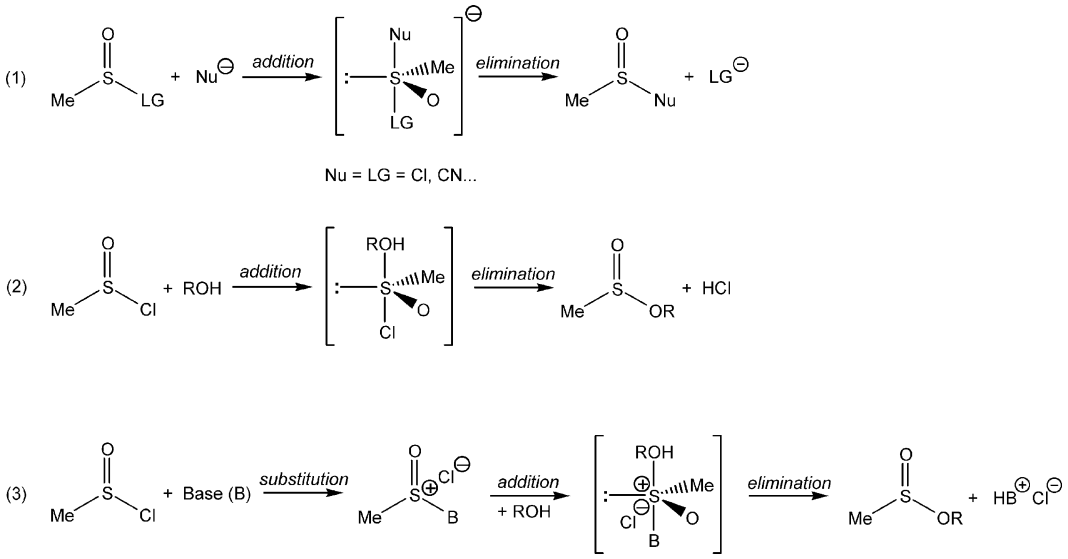

Dramatic effects of the base upon stereoselectivity have been observed for both the DAG method and the cinchona-assisted DKR. In the former case, the diastereoselection sense can be easily changed using different nonchiral bases. For instance, pyridine and Hunig's base gave rise to different diastereomers.[20−22] In the latter case, the structure of the catalytic chiral base has an important influence upon the optical purity of the final reaction product.[16,17] These experimental results suggested that the base not only catalyzes the inversion of the sulfinyl chloride but also participates in the formation of the new S−OR bond. To the best of our knowledge, the mechanistic details behind these base effects are unknown. Computational studies have been helpful for the clarification of the mechanism of the metal-assisted oxidation of sulfides,[11−13,42] and in this work, we will apply them to systems related to DKR of sulfinyl chloride racemates.

Nucleophilic substitution at sulfur has been theoretically studied by Bachrach.[43,44] In a recent study, this reaction was explored for the particular case of sulfinyl chlorides.[45] The reaction was modeled considering the nucleophilic substitution at sulfur of methanesulfinyl derivatives by small anions identic to the leaving group. In most cases the reaction was found to follow an addition−elimination mechanism involving the formation of a 10-S-4 hypervalent sulfur intermediate (mechanism 1 in Scheme 3). This proposal is a good starting point for the analysis of the Cl substitution by RO in the DKR of sulfinyl chlorides, but the simplicity of the model does not allow the consideration of some key issues such as the role of the base, which is essential in the enantioselective process.

In the present work, we formulate and study an analogous mechanism for the reaction in which ROH reacts with methyl sulfinyl chloride to give the corresponding sulfinate ester. This reaction pathway will be referred throughout this article as the neutral mechanism, because it formally does not imply charge separation (mechanism 2 in Scheme 3). An additional possibility previously proposed by some of us[22] implies initial substitution of Cl by the base. This reaction pathway will be to referred throughout this article as the ion pair mechanism because it formally involves charge separation (mechanism 3 in Scheme 3). The addition step in which the absolute configuration of the sulfinate ester product is defined was explored in detail, and the role of the base in the formation of the S−OR bond was clarified. The mechanistic insight provided by our study is relevant for both the DAG method and the cinchona-assisted DKR.

Computational Details

All results reported in this paper were obtained using the hybrid Becke3LYP density functional[46,47] as implemented within the Gaussian03 program.[48] The 6−31g(d) basis set[49,50] was used for oxygen, nitrogen, carbon, and hydrogen. Effective core potentials were used to replace the 10 innermost electrons of sulfur and chlorine,[51] as we did in our previous article,[41] to unify the conclusions of both studies. The valence double-ζ basis set associated to the pseudopotential in the program[48] with the contraction labeled as LANL2DZ was used for these two elements, supplemented with a d shell.[52]

(42) Sensato, F. R.; Custodio, R.; Longo, E.; Safont, V. S.; Andres, J. *Eur. J. Org. Chem.* **2005**, *11*, 2406.
(43) Bachrach, S. M.; Woody, J. T.; Mulhearn, D. C. *J. Org. Chem.* **2002**, *67*, 8983.
(44) Hayes, J. M.; Bachrach, S. M. *J. Phys. Chem. A* **2003**, *107*, 7952.
(45) Norton, S. H.; Bachrach, S. M.; Hayes, J. M. *J. Org. Chem.* **2005**, *70*, 5896.
(46) Becke, A. D. *J. Chem. Phys.* **1993**, *98*, 5648.
(47) Lee, C.; Parr, R. G.; Yang, W. *Phys. Rev. B: Condens. Matter Mater. Phys.* **1988**, *37*, 785.
(48) Frisch, M. J.; Trucks, G. W.; Schlegel, H. B.; Scuseria, G. E.; Robb, M. A.; Cheeseman, J. R.; Montgomery, J. A., Jr.; Vreven, T.; Kudin, K. N.; Burant, J. C.; Millam, J. M.; Iyengar, S. S.; Tomasi, J.; Barone, V.; Mennucci, B.; Cossi, M.; Scalmani, G.; Rega, N.; Petersson, G. A.; Nakatsuji, H.; Hada, M.; Ehara, M.; Toyota, K.; Fukuda, R.; Hasegawa, J.; Ishida, M.; Nakajima, T.; Honda, Y.; Kitao, O.; Nakai, H.; Klene, M.; Li, X.; Knox, J. E.; Hratchian, H. P.; Cross, J. B.; Bakken, V.; Adamo, C.; Jaramillo, J.; Gomperts, R.; Stratmann, R. E.; Yazyev, O.; Austin, A. J.; Cammi, R.; Pomelli, C.; Ochterski, J. W.; Ayala, P. Y.; Morokuma, K.; Voth, G. A.; Salvador, P.; Dannenberg, J. J.; Zakrzewski, V. G.; Dapprich, S.; Daniels, A. D.; Strain, M. C.; Farkas, O.; Malick, D. K.; Rabuck, A. D.; Raghavachari, K.; Foresman, J. B.; Ortiz, J. V.; Cui, Q.; Baboul, A. G.; Clifford, S.; Cioslowski, J.; Stefanov, B. B.; Liu, G.; Liashenko, A.; Piskorz, P.; Komaromi, I.; Martin, R. L.; Fox, D. J.; Keith, T.; Al-Laham, M. A.; Peng, C. Y.; Nanayakkara, A.; Challacombe, M.; Gill, P. M. W.; Johnson, B.; Chen, W.; Wong, M. W.; Gonzalez, C.; Pople, J. A. *Gaussian 03*, revision C.02; Gaussian, Inc.: Wallingford, CT, 2004.
(49) Hehre, W. J.; Ditchfield, R.; Pople, J. A. *J. Phys. Chem.* **1972**, *56*, 2257.
(50) Hariharan, P. C.; Pople, J. A. *Theor. Chim. Acta* **1973**, *28*, 213.
(51) Wadt, W. R.; Hay, P. J. *J. Chem. Phys.* **1985**, *82*, 284.

All geometries reported in this article were fully optimized in the gas phase without imposing geometrical constraints. The stationary points located in the potential energy hypersurface were identified as true minima or transition states by vibrational analysis. The reactants and products directly connected to the transition states were located through IRC calculations.[53,54]

The electronic structure of each stationary point was analyzed by inspecting the atomic partial charges. The Mulliken populations were used for this purpose, although they are not the best approach. Charge separation was present along the computed reaction pathways, and solvent effects were thus considered by means of the CPCM method.[55] The geometries of the intermediates and transition states found in gas phase should be, in principle, reoptimized at the CPCM level. Nevertheless, we assumed that the structures of these stationary points are not strongly affected by the solvent, and the free energies of solvation were evaluated through single-point CPCM calculations (G_{CPCM}) on the gas-phase optimized geometries. All reported energy values correspond to free energies in solution (G_{sol}) considering the solvent used in most experiments: toluene ($\epsilon = 2.379$). The values of G_{CPCM} account for the free energies of solvation but without including the thermal and entropy contributions of the solute. These contributions were computed as the difference between the potential and free energies of the solute in gas phase ($G_g - E_g$) found in the vibrational analysis and added to G_{CPCM} to obtain G_{sol} (see eq 1). The absolute values of E_g, G_g, G_{CPCM}, and G_{sol} of all stationary points are given in the Supporting Information.

$$G_{sol} = G_{CPCM} + (G_g - E_g) \quad (1)$$

The alcohols and tertiary amines used in the DKR of sulfinyl chlorides (DAG and cinchona-assisted DKR synthetic methods) were modeled as methanol and trimethylamine, respectively. This model constitutes a drastic simplification of the real catalytic systems and implies the loss of enantioselectivity because chirality is supressed. Nevertheless, the main electronic effects governing the reaction mechanism are conserved.

The stationary points found along the neutral and ion pair mechanisms were identified with the NM and IPM labels, respectively. The "ba" prefix (standing for base-assisted) was introduced to identify the geometries belonging to those pathways in which an extra molecule of base was added to the system. Arabic numbers were used to distinguish between the different structures of a given path. The reactant-side, transition state, and product-side geometries were labeled as 0, 1, and 2, respectively. For example, **baNM1** is the transition state of the base-assisted neutral mechanism and **IPM2** is the product-side intermediate in the nonassisted ion-pair mechanism.

Results and Discussion

Neutral Mechanism. The neutral mechanism, in which methyl sulfinyl chloride (MSC) reacts with methanol, was characterized through calculation of the corresponding transition state and intermediates. The **NM1** transition state (see Figure 1) corresponds to the addition of methanol to MSC. The unique, imaginary frequency found for this stationary point revealed that this addition is coupled with the elongation of the S−Cl bond and a hydrogen transfer between the oxygens of methanol (O1) and MSC (O2). In fact, we were not able to localize any transition state involving the formation of the S−O1 bond without such hydrogen transfer. **NM1** is a saddle point in which the movement of up to five different atoms, O1, S, O2, H, and Cl, participates in the transition vector. Relaxation of **NM1** toward reactants and products by IRC calculations gave rise to intermediates **NM0** and **NM2**, respectively.

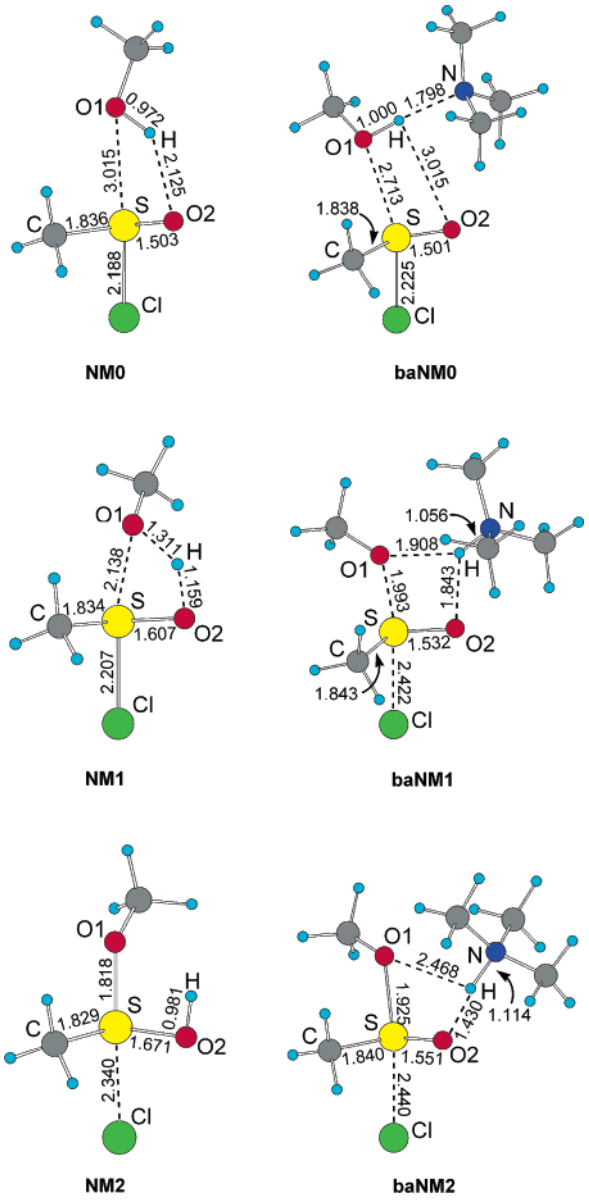

FIGURE 1. Becke3LYP-optimized stationary points for the nonassisted (left) and base-assisted (right) neutral mechanisms.

Methanol and MSC appear associated in the reactant-side intermediate **NM0** by an OH···O hydrogen bond with a H··· O2 distance of 2.125 Å. From **NM0** to **NM1**, the O1−S distance is shortened from 3.015 to 2.138 Å whereas the S−Cl distance is elongated from 2.188 to 2.207 Å. These geometrical parameters indicate that the O1−S bond is being formed while the S−Cl bond, standing trans to the former, is elongated. Moreover, the O1−H bond is elongated from 0.972 to 1.311 Å whereas O2−H is dramatically shortened from 2.125 to 1.159 Å. The evolution of these distances is consistent with a hydrogen-transfer process between O1 and O2. The plane defined by the three atoms involved in such process (O1, H, and O2) also contains the S atom, as indicated by the H−O2−S−O1 dihedral angle of −1.7°. In the product-side intermediate,

(52) Höllwarth, A.; Böhme, M.; Dapprich, S.; Ehlers, A. W.; Gobbi, A.; Jonas, V.; Köhler, K. F.; Stegmann, R.; Veldkamp, A.; Frenking, G. *Chem. Phys. Lett.* **1993**, *208*, 237.
(53) Gonzalez, C.; Schlegel, H. B. *J. Chem. Phys.* **1989**, *90*, 2154.
(54) Gonzalez, C.; Schlegel, H. B. *J. Phys. Chem.* **1990**, *94*, 5523.
(55) Barone, V.; Cossi, M. *J. Phys. Chem. A* **1998**, *102*, 1995.

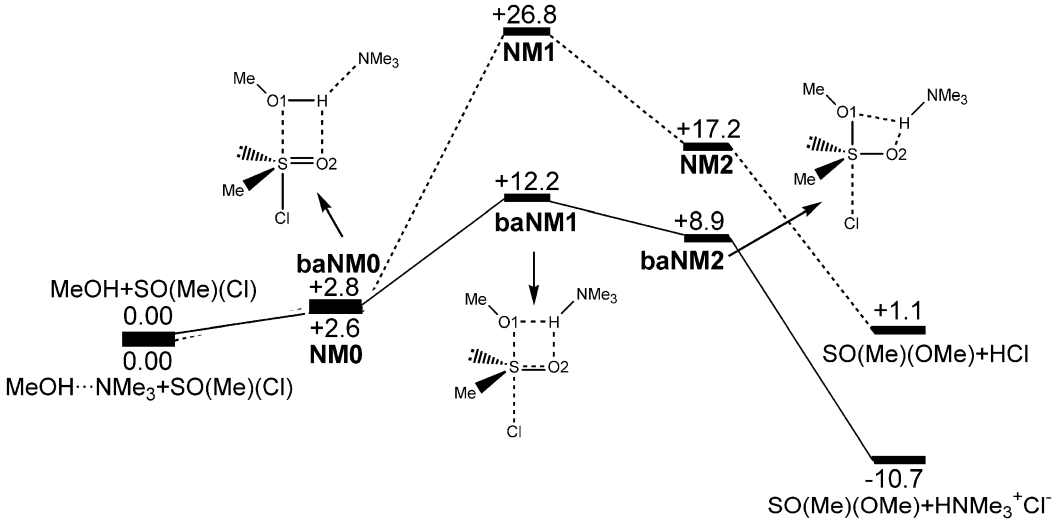

FIGURE 2. Free energy profiles for the nonassisted (dashed line) and base-assisted (solid line) neutral mechanisms.

NM2, O1 is clearly bound to S with a S−O1 bond distance of 1.818 Å, and the acidic hydrogen of methanol appears completely transferred to the sulfinyl oxygen (O2), as the O2−H distance of 0.981 Å indicates. Furthermore, the S−Cl bond is elongated to 2.340 Å in **NM2**. The S−O2 bond is also elongated as it is transformed from a double S═O bond in **NM0** (1.503 Å) to a single S−OH bond in **NM2** (1.671 Å) through the **NM1** transition state (1.607 Å). All of these data have two possible interpretations: (1) the reaction is a S_N2 nucleophilic substitution in which methanol acts as the nucleophile and Cl as the leaving group (cleavage of the S−Cl bond) or (2) the reaction consists of an addition in which the binding of methanol to sulfur gives rise to a hypervalent 10-S-4 intermediate, namely **NM2** (conservation of the S−Cl bond). In any case, the relevant issue is that the reaction involves the formation of a new S−OMe bond coupled with a hydrogen transfer from methanol to MSC.

The relationship of **NM0** with the separate reactants is obvious, because it is simply a long distance adduct of both molecules. The connection of **NM2** to the products is slightly more ellaborated but also straightforward. The transition state corresponding to the elimination step in which **NM2** is transformed into SO(Me)(OMe) and HCl (second step of mechanism 2 in Scheme 3) was computed. The transition vector of this saddle point consists of the rotation of the S−O2H bond coupled with the cleavage of the O2−H bond and the formation of a new H−Cl bond. The rotation of the S−O2H bond is also accompanied by the cleavage of the S−Cl bond and the shortening of the S−O1 bond. The free energy in solution of this structure is 19.1 kcal/mol, clearly lower than that found for the previous transition state (26.8 kcal/mol). On the other hand, the stereochemical outcome of the reaction is decided by the addition because the absolute configuration of sulfur is retained in the elimination. All these data pointed out that the key step of the mechanism is the addition of methanol to MSC through the transition state **NM1**, and the elimination step was thus not further explored.

The structures of **NM0**, **NM1**, and **NM2** consist of distorted trigonal bipyramids (see Figure 1). The equatorial plane is occupied by C, O2, and the lone electron pair of sulfur, whereas O1 and Cl are in the axial positions. These structural features are clearly reflected on the geometrical parameters. In **NM2**, for instance, O2 and C are found in the equatorial plane with a C−S−O2 angle of 103.2°. On the other hand, O1 and Cl lay in the axial positions with a O1−S−Cl angle of 176.0°. The O1−S−Cl axis is perpendicular to the equatorial plane as shown by the C−S−O2−O1 and C−S−O2−Cl dihedral angles of −88.9° and 88.4°, respectively. The other possible isomers of the trigonal bipyramid were explored without success. In all cases, the corresponding transition state was not found or had higher energy in comparison with **NM1**. The racemization of **NM2** through Berry pseudorotations was also explored, but the corresponding transition states were not found.

TABLE 1. Mulliken Charges of Chlorine (q_{Cl}) in the Neutral Mechanism

nonassisted	q_{Cl} (au)	base-assisted	q_{Cl} (au)
NM0	−0.240	**baNM0**	−0.293
NM1	−0.261	**baNM1**	−0.492
NM2	−0.407	**baNM2**	−0.507

In **NM2**, the S−Cl bond appears clearly elongated (2.340 Å) with respect to reactants (2.188 Å in **NM0**). Such separation suggests some degree of ion-pair character for **NM2** that could be formulated as $S(OH)(Me)(OMe)^+Cl^-$. This possibility was confirmed by inspection of the Mulliken charge of Cl (q_{Cl}). The values of q_{Cl} collected in Table 1 show that all along the reaction pathway, chlorine has a partial negative charge that increases. From **NM0** to **NM1**, the polarization of the system is small and almost constant as the values of q_{Cl} (−0.240 au in **NM0** and −0.261 au in **NM1**) point out. In contrast with this, q_{Cl} increases up to −0.407 au with the formation of **NM2** intermediate. The polarization of **NM2** is coupled with the elongation of the S−Cl bond commented on above. We can thus conclude that there is a significant degree of charge separation even in the neutral mechanism. This phenomenon suggests the necessity of introducing solvent effects, and we did it using the CPCM method.

The profile of free energy in solution was computed for the neutral mechanism (see Figure 2). The formation of **NM0** is endergonic by 2.6 kcal/mol. This process implies the binding of methanol with MSC through a hydrogen bond, which should be stabilizing, but the formation of **NM0** is disfavored by its bimolecular associative nature, which involves entropy loss. The relative energies of **NM1** and **NM2** are also affected by this unfavorable entropic effect because both stationary points also

involve the association of methanol with MSC. The most relevant result is that the addition transition state, **NM1**, stands well above reactants at 26.8 kcal/mol. The energy of **NM2** with respect to reactants (17.2 kcal/mol) points out the poor stability of this intermediate. The high energy of transition state **NM1** is likely associated to the strained nature of the S···O1···H···O2···S arrangement. The optimal geometry for proton transfer would have O1, H, and O2 in a straight line, but this is not compatible with the simultaneous formation of the S−O1 bond and with the fact that O2 is also bound to S. Overall, the reaction is slightly endergonic by 1.1 kcal/mol.

Base-Assisted Neutral Mechanism. The hydrogen transfer between O1 and O2 involved in the addition of methanol to MSC was the key step in the neutral mechanism. This finding suggests that the base may participate in the reaction, assisting such hydrogen transfer with an OH···N interaction. This possibility was scrutinized by reoptimizing the structure of the transition state found for the neutral mechanism, **NM1**, adding a molecule of NMe_3 attached to the hydrogen being transferred. Such optimization converged into the **baNM1** geometry (see Figure 1). From the structural point of view, **baNM1** is more product-like than **NM1**, as reflected by the shorter S−O1 (1.993 Å) and longer S−Cl (2.422 Å) distances. But the most relevant structural change is that the transferred hydrogen appears now clearly bound to the nitrogen of the base, with a N−H distance of 1.056 Å. Taking **NM1** as reference, it is clear that the base pulls this hydrogen atom away from both O1 and O2, as proven by the longer O1−H and O2−H distances in **baNM1** (1.908 and 1.843 Å, respectively).

The transition vector of **baNM1** consists of the S−O1 bond formation coupled with the elongation of S−Cl, as previously found for **NM1**. The main novelty found in **baNM1** is that the nitrogen of the base also participates in the transition vector bound to H and following its movement. As in **NM1**, the atoms directly involved in the hydrogen transfer (O1, H, O2, and now also N) are coplanar with S, as indicated by the H−O2−S−O1 and S−O2−H−N dihedral angles of −12.8 and 167.3°, respectively. The IRC of **baNM1** toward reactants converged into **baNM0** in which H appears strongly bound to O1. In contrast with this, on the other side of the reaction (**baNM2**), H appears bound to N suggesting the basicity relationship O1 > N > O2.

In **baNM0**, methanol is bound to NMe_3 by a hydrogen bond as indicated by the H···N distance of 1.798 Å. The long S−O1 and H−O2 distances found in **baNM0** (2.713 and 3.015 Å, respectively) point out that this species can be considered as a complex of MeOH···NMe_3 associated with MSC. As the reaction coordinate evolves from **baNM0** to **baNM2**, the S−O1 distance is shortened from 2.713 to 1.925 Å, whereas the S−Cl bond is elongated from 2.225 to 2.440 Å. These structural data reflects the formation of the S−O1 bond coupled with the elongation of the S−Cl bond. Simultaneously, the S−O2 bond is elongated from 1.501 to 1.551 Å. In the product-side intermediate, **baNM2**, the base is protonated and bound to O2 through a hydrogen bond as indicated by the H···O2 distance of 1.430 Å. In summary, we can conclude that the main structural change introduced by the participation of the base in the neutral mechanism is that the transferred hydrogen is bound to the base in the addition transition state.

As in **NM2**, the long S−Cl bond found in **baNM2** indicates that the hypervalent 10-S-4 character of sulfur in this intermediate is arguable. This species can be rather considered as a 8-S-3 ion pair with the formula (Me)(MeO)SO···$HNMe_3^+Cl^-$. The electronic structure of this species, and of **baNM0** and **baNM1** as well, was inspected considering the partial charge of chlorine (q_{Cl}). The values collected in Table 1 show that the negative charge of chlorine rises all along the reaction pathway from −0.293 au in **baNM0** to −0.507 au in **baNM2** through −0.492 au in **baNM1**. The combination of this polarization with the elongated S−Cl bonds, specially long in **baNM1** (2.422 Å) and **baNM2** (2.440 Å), shows that the mechanism involves substantial charge separation. Comparison with the q_{Cl} values found for **NM0**, **NM1**, and **NM2** reveals that the participation of the base increases the polarization of all stationary points and especially of the addition transition state.

The profile of free energy in solution for the **baNM0** → [**baNM1**]‡ → **baNM2** pathway was computed and represented in Figure 2. As for **NM0**, the formation of **baNM0** is moderately endergonic by 2.8 kcal/mol, probably due to the bimolecular associative nature of this process. For the same reason, the association of NMe_3 to methanol giving rise to MeOH···NMe_3 is also endergonic, in this case by 7.5 kcal/mol. The addition transition state, **baNM1**, stands 12.2 kcal/mol above reactants whereas the product intermediate, **baNM2**, is less stable than reactants by 8.9 kcal/mol. Overall, the reaction is exergonic by −10.7 kcal/mol.

The comparison between the energy profiles represented in Figure 2 reveals that with NMe_3 there is a lower energy path involving a more stable transition state and product-side intermediate. The base decreases the relative energy of the addition transition state from 26.8 to 12.2 kcal/mol, thus reducing the energy barrier by 14.6 kcal/mol. The main role of the base in **baNM1** is to relax the strain present in the S···O1···H···O2···S arrangement of **NM1**. As can be observed in Figure 1, the presence of trimethylamine allows the proton to stay further away from both O1 and O2, which can in turn get closer to the sulfur center, thus forming a much less strained four-member ring. Furthermore, the formation of a strong N−H bond between the transferred hydrogen and the base also contributes to the reduction of the addition energy barrier. The ability of external basic centers to assist intramolecular proton transfers has been previously reported for enolization processes.[56] The participation of the base also increases the relative stability of the product-side intermediate by 8.3 kcal/mol. This effect is probably due to the substitution of the O2−H bond of **NM2** by the O2···H−N bonds found in **baNM2**. Furthermore, the base makes the overall reaction exergonic through the formation of the $HNMe_3^+Cl^-$ ion pair.

Interestingly, in the transition state **baNM1**, the base stands next to the site in which the new S−OR bond is formed. Thus, through this mechanism, the base might be able to influence enantioselectivity in the real systems,[57] by means of stereoelectronic interactions between a nonchiral alcohol and an optically active base (cinchona-assisted DKR[16,17]) or between a nonchiral base and an optically active OR fragment (DAG method[20−22]).

Ion Pair Mechanism. Taking the same reactants of the base-assisted neutral mechanism, SO(Me)(Cl) + MeOH + NMe_3, it is possible to consider a different reaction pathway in which the base initially displaces chlorine, giving rise to an ion pair with the formula SO(Me)$(NMe_3)^+Cl^-$ (see Scheme 3). This ion

(56) Rodriguez-Santiago, L.; Vendrell, O.; Tejero, I.; Sodupe, M.; Bertran, J. *Chem. Phys. Lett.* **2001**, *334*, 112.

(57) Lipkowitz, K. B.; D'Hue, C. A.; Sakamoto, T.; Stack, J. N. *J. Am. Chem. Soc.* **2002**, *124*, 14255.

pair might undergo addition of methanol as MSC does in the neutral mechanisms described above.

The stationary point **IPM1** corresponds to the addition transition state of the ion pair mechanism. As in the neutral mechanisms, the hydrogen of methanol stands between the oxygens of methanol (O1) and MSC (O2), as reflected by the O1−H and O2−H distances of 1.220 and 1.258 Å respectively. These structural data suggests that the addition is coupled with a hydrogen transfer, a point confirmed by the transition vector found in the vibrational analysis. In this vector, the hydrogen transfer is coupled with the formation of the S−O1 bond and the rupture of the S−N bond lying trans to it.

The IRC-driven relaxation of **IPM1** to the reactant and product sides of the reaction converged into **IPM0** and **IPM2**, respectively. The initial intermediate, **IPM0**, is a complex of methanol associated with Cl···SO(Me)(NMe_3) characterized by long S−O1 and H−O2 distances. The formation of **IPM0** involves the initial substitution of Cl by NMe_3 (first step of mechanism 3 in Scheme 3). This step was not studied in detail because, as will be commented on below, the addition of methanol to **IPM0** follows a reaction pathway higher in energy than the neutral mechanism. The product intermediate, **IPM2**, is a complex of NMe_3 associated with Cl···SOH(Me)(OMe). From **IPM0** to **IPM2**, the S−O1 bond is shortened from 2.607 to 1.687 Å, whereas the S−N bond is elongated from 2.194 to 2.735 Å. The variation of these distances indicate the formation of the S−O1 coupled with the cleavage of the S−N bond. Simultaneously, H is transferred from O1 to O2 as the O1−H (0.970 Å in **IPM0**) and O2−H (0.976 Å in **IPM2**) point out. Moreover, the S−O2 bond is elongated from 1.509 Å in **IPM0** to 1.736 Å in **IPM2** as it is transformed from a double to a single bond. The shortest S−Cl distance is found in **IPM2** with a value of 2.583 Å, clearly longer than that of MSC (2.199 Å). These distances indicate that the S−Cl bond is completely elongated all along the ion pair mechanism. The structural transformations found in the **IPM0** → [**IPM1**]‡ → **IPM2** pathway are analogous to those found in the neutral mechanisms: the formation of the S−O1 and O2−H bonds is accompanied by the rupture of the O1−H bond and the bond standing trans to S−O1, which now is a S−N bond.

The geometry of all stationary points involved in the reaction pathway is an octahedron with the sulfur lone electron pair occupying one of the sites. C is trans to the lone pair of sulfur, O1 is trans to N, and O2 is trans to Cl. In **IPM2**, for instance, the latter trans relationships are clearly indicated by the O1−S−N and O2−S−Cl bond angles of 174.1 and 178.1°, respectively. Furthermore, all bond angles between the fragments in cis were very close to 90°, with the largest deviation given by O1−S−C (93.9°).

As found for the neutral mechanisms, the 10-S-4 hypervalency in the product-side intermediate, **IPM2**, is arguable and both the S−Cl and S−N bonds appear clearly elongated in this species. **IPM2** can be formulated as an ion pair constituted by the Me_3N···SOH(Me)(OMe)$^+$ cation and the Cl^- counteranion. The ion pair character of the stationary points found along the ion pair mechanism was explored in more detail analyzing the evolution of the chlorine partial charges (see Table 2). The values of q_{Cl} decrease along the reaction pathway from −0.686 au (**IPM0**) to −0.565 au (**IPM2**) through −0.648 au (**IPM1**), as the S−Cl bond distance also decreases. These results reveal that charge separation is reduced along the ion pair mechanism. Nevertheless, the partial negative charges of Cl in all stationary points are clearly higher than those found in the neutral mechanisms. The largest difference is found between **NM0** and **IPM0** with a Δq_{Cl} of allmost half electron (0.446 au). These data confirm the higher ion pair character of the **IPM0** → [**IPM1**]‡ → **IPM2** pathway in comparison with the neutral mechanisms. On the other hand, these results highlight again the necessity of introduction of solvent effects included in our model of the reaction.

TABLE 2. Mulliken Partial Charges of Chlorine (q_{Cl}) in the Ion-Pair Mechanism

nonassisted	q_{Cl} (au)	base-assisted	q_{Cl} (au)
IPM0	−0.686	**baIPM0**	−0.689
IPM1	−0.648	**baIPM1**	−0.721
IPM2	−0.565	**baIPM2**	−0.635

The profile for the free energy in solution of the ion pair mechanism is represented in Figure 4. The formation of the initial intermediate, **IPM0**, is endergonic by 17.7 kcal/mol. The energy barrier from the separated reactants to **IPM1** is 40.9 kcal/mol. The product intermediate is also less stable than reactants

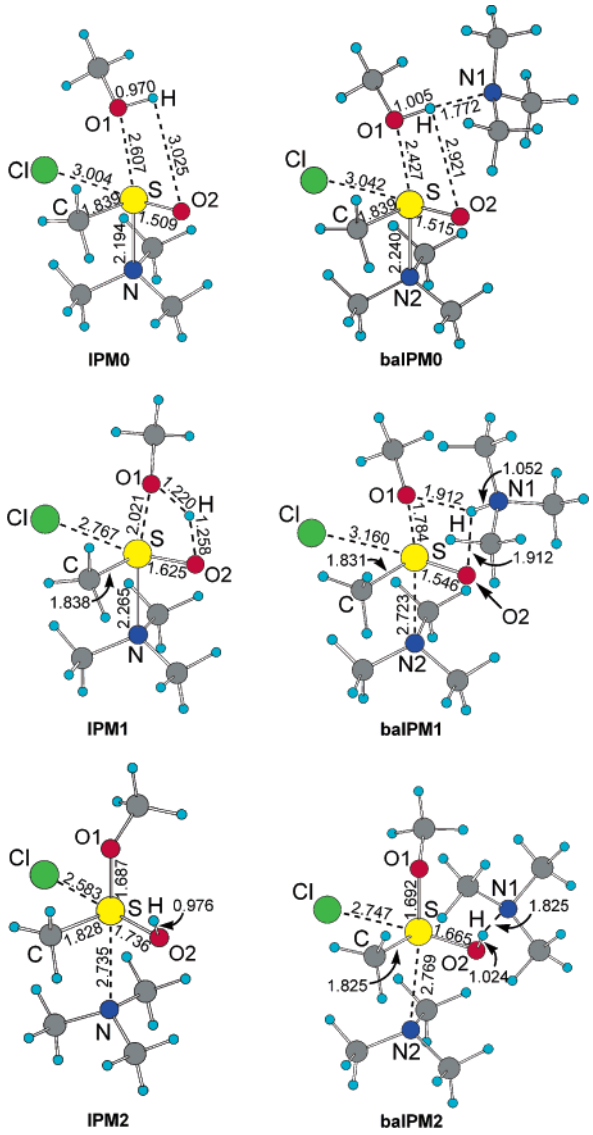

FIGURE 3. Becke3LYP-optimized stationary points for the nonassisted (left) and base-assisted (right) ion-pair mechanisms.

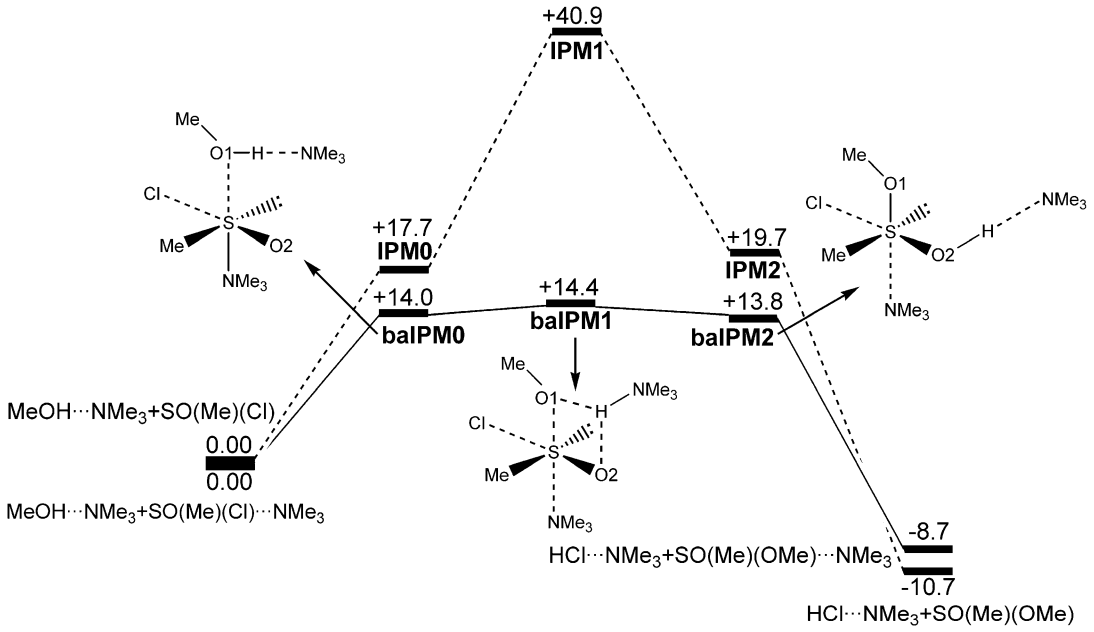

FIGURE 4. Free energy profiles for the nonassisted (dashed line) and base-assisted (solid line) ion-pair mechanisms.

by 19.7 kcal/mol, and the overall reaction is exergonic by 10.7 kcal/mol. The comparison of the energy profiles calculated for the nonassisted neutral (see Figure 2) and ion pair mechanisms reveals that the latter mechanism is clearly higher in energy. The intermediates, **IPM0** and **IPM2**, are 15.1 and 2.5 kcal/mol less stable than **NM0** and **NM2** respectively. The largest difference was found in the addition barrier, which is increased from 26.8 kcal/mol in the neutral mechanism to 40.9 kcal/mol in the ion pair mechanism. Interestingly, the largest rise in the values of q_{Cl} corresponds to the reactant-side intermediate (0.446 au from **NM0** to **IPM0**; see Tables 1 and 2) and the transition state (0.387 au from **NM1** to **IPM1**; see Tables 1 and 2), which in turn are the species that undergo the most important rise in their relative energies. Thus, the high relative energies of the stationary points involved in the ion pair mechanism can be assigned to the high degree of charge separation found for this mechanism, which is poorly favored by the very low polarity of the solvent, toluene.

The energy profile found for **IPM0** → [**IPM1**]‡ → **IPM2** shows that the ion pair mechanism is clearly less favored than the base-assisted neutral mechanism. We can thus conclude that the main role of the base in assisting this reaction is not the initial displacement of chloride from the coordination sphere of sulfur. Furthermore, in **IPM1**, NMe_3 is in trans position with respect to methanol, far from the site of chemistry in which the new S−O1 bond is formed. With such a scenario, it is difficult to figure out how the base is able to influence enantioselectivity as it has been experimentally observed.[16,17,20−22]

Base-Assisted Ion Pair Mechanism. As in the nonassisted neutral mechanism, in the ion pair mechanism, the addition of methanol to MSC is coupled with a hydrogen transfer between O1 and O2. This suggests that the same catalytic effect of the base found for the neutral mechanism is also possible for the ion pair mechanism. This possibility was explored recomputing the addition transition state **IPM1** introducing an additional molecule of NMe_3 in close proximity to the transferred hydrogen. This calculation converged into the transition state **baIPM1** (see Figure 3). In the transition vector of this saddle point, the S−O1 bond is contracted whereas the S−NMe_3 is elongated, and simultaneously H is transferred from O1 to O2. The movement of H is followed by the additional molecule of NMe_3, which appears clearly bound to H with a N1−H bond distance of 1.052 Å. Hence, an additional molecule of trimethylamine can participate in the ion pair mechanism assisting the hydrogen transfer as already found for the neutral mechanism.

The IRC relaxation of **baIPM1** toward reactants converged into **baIPM0** (see Figure 3). This species is a complex of SO(Cl)(Me)(NMe_3) with methanol, which in turn is bound to NMe_3 by a hydrogen bond with a H···N1 distance of 1.772 Å. As the reaction coordinate evolves from **baIPM0** to **baIPM1**, the S−O1 bond is shortened from 2.427 to 1.784 Å and the S−NMe_3 bond is elongated from 2.240 to 2.723 Å. Furthermore, the O1−H bond is elongated from 1.005 to 1.912 Å whereas the O2−H bond is shortened from 2.921 to 1.912 Å. These results indicate the formation of the S−O1 bond and the rupture of S−NMe_3, coupled with a hydrogen transfer from O1 to O2. In contrast with **IPM1**, in **baIPM1**, the bond between sulfur and the base is much more elongated in the transition state. As found in **baNM1**, the close proximity between NMe_3 and the reactive center in which the S−O1 bond is formed is consistent with the strong base effects on enantioselectivity experimentally observed.[16,17,20−22]

In the product-side intermediate, **baIPM2**, the S−O1 (1.692 Å) and O2−H (1.024 Å) bonds are formed whereas S−NMe_3 (2.769 Å) is broken. In contrast with **baNM2**, the molecule of NMe_3 assisting the hydrogen transfer is not bound to H but instead making a hydrogen bond with it, as the N1···H distance of 1.825 Å points out. The hypervalence is again avoided by the rupture of the S−NMe_3 bond, and **baIPM2** is formally a 8-S-3 sulfur compound.

As in the nonassisted ion pair mechanism, the geometry around sulfur is octahedral all along the reaction pathway. This feature can be clearly observed in **baIPM2**, in which O1, S, and N2 form an axis with a O1−S−N2 angle of 173.8°, perpendicular to a square plane occupied by S, O2, C, Cl, and the lone electron pair of sulfur. The coplanarity of S, O2, C, and Cl is indicated by the Cl−S−C−O2 dihedral angle of

173.0°, whereas the perpendicular arrangement between the S,-O2,C,Cl plain and the O1−S−N2 axis is reflected on the O2−S−C−O1 and O2−S−C−N2 dihedral angles of 97.7 and −88.3°, respectively. Other possible octahedral isomers were also explored without success.

The long S−Cl distances found in the transition state and intermediates, longer than 2.700 Å in all cases, suggests a strong ion pair character for all these species in which Cl would act as counteranion. This possibilty was explored analyzing the evolution of the Mulliken partial charges of chlorine (q_{Cl}). The values collected in Table 2 show that Cl has a negative partial charge that reaches a maximum value in the transition state. The charges are in general higher than in the nonassisted ion pair mechanism with the largest difference given by the transition state. In fact, **baIPM1** has the largest value of q_{Cl} among all stationary points found in our mechanistic study. Not surprisingly, it also has the longest S−Cl distance (3.160 Å).

The profile of free energy in solution of the reaction was calculated and is presented in Figure 4. As already found in all other mechanisms, the reactant intermediate, **baIPM0**, is less stable than reactants, in this case by 14.0 kcal/mol. In comparison with **IPM0**, this intermediate is 3.7 kcal/mol more stable. The addition transition state implies an energy barrier of 14.4 kcal/mol, clearly lower than the barrier given by **IPM1**, 40.9 kcal/mol. We can thus conclude that the base reduces the barrier of the addition by assisting the hydrogen transfer between O1 and O2. The barrier reduction of 26.5 kcal/mol is clearly larger than that of the neutral mechanism (14.6 kcal/mol). These results indicate that the higher degree of ion pair character stimulates the effect of the base. The product intermediate is less stable than reactants by 13.8 kcal/mol and the **baIPM0** → [**baIPM1**]‡ → **baIPM2** profile is very flat. The overall reaction is exergonic by 8.7 kcal/mol.

The comparison of all the energy profiles presented above (see Figures 2 and 4) demonstrates that both the neutral and ion pair mechanisms are assisted by NMe_3, which helps the hydrogen transfer involved in the addition of methanol to MSC. The base-assisted neutral and ion pair pathways are hence the most favored reaction mechanisms. The comparison of the energy profiles for these two mechanisms indicates that base-assisted neutral mechanism is the lowest energy pathway for the substitution of Cl by MeO. The differences in their energy barriers is too small to discard completely the ion pair possibility, but it must be taken into account that it ought to be further disfavored by bulkier bases.

Conclusions

The rate-determining step of the nucleophilic substitution of chloride by alkoxy in sulfinyl derivatives goes through a transition state where the formation of the S−OR bond and the elongation of the S−Cl bond take place simultaneously. In this key step, the acidic hydrogen of the alcohol is transferred to the oxo group attached to sulfur. The barrier for this step is quite high in the absence of external molecules but is substantially lowered (by more than 10 kcal/mol) by the presence of a base, which stabilizes the proton being transferred. This is thus the main role of the base in this process. A second base molecule could also act by displacing the chlorine in the initial step of the reaction, but the computed barriers for this base-assisted ion-pair mechanism are slightly higher. Interestingly, the base molecule bound to hydrogen stands next to the site where the S*O(Me)(OR) chiral center is formed. Hence, the present study on a model system constitutes a promising first step toward the rationalization of the interesting effects of the base upon enantioselectivity found in the cinchona-assisted DKR[16,17] and the DAG method.[20−22] The origin of these base effects are being currently explored in our laboratory with a QM/MM study on the base-assisted neutral mechanism considering the real system.

Acknowledgment. Financial support from the ICIQ foundation and the Spanish MEC through Projects CTQ2005-09000-CO1-02, CTQ2005-09000-CO1-01, and BQU2003-00937 and from the Catalan DURSI through projects 2005SGR00715 and 2005SGR00896 is acknowledged. G.U. acknowledges the Spanish MEC for a "Ramón y Cajal" contract.

Supporting Information Available: Cartesian coordinates, number of imaginary frequencies and absolute potential, CPCM, solvation and Gibbs free energies of all stationary points reported in the text. This material is available free of charge via the Internet at http://pubs.acs.org.

JO060546P